Journal of Hydrology 631: 130768 (2024)

Combining isotopic and elemental tracers for enhanced sediment source partitioning in complex catchments

Ivan Lizaga [a]*, Borja Latorre [b], Samuel Bodé [a], Leticia Gaspar [b], Pascal Boeckx [a], Ana Navas [b]

a Isotope Bioscience Laboratory - ISOFYS, Department of Green Chemistry and Technology, Ghent University, Coupure Links 653, 9000, Gent, Belgium
b Estación Experimental de Aula-Dei (EEAD-CSIC), Spanish National Research Council, Zaragoza, Spain. Avenida Montañana, 1005, 50059 Zaragoza, Spain.

Abstract

Sediment fingerprinting has the potential to elucidate and quantify soil erosion processes by assessing the provenance of sediments in water bodies. In this regard, several types of tracers have been used to discriminate different sediment sources. Stable isotopic composition of fatty acids is associated with land use/vegetation cover, while elemental composition is related to different mineralogy. Isotopic tracers are characterised by their isotopic ratio and total content, requiring specific fingerprinting models. Consequently, this has led to few studies combining elemental and isotopic tracers.

In this context, our analysis focuses on the ability of merging isotopic and elemental tracers to distinguish sediment sources in an ungauged Mediterranean mountain catchment. This catchment is characterised by homogenous lithology, ephemeral streams, and a marked seasonality. It has experienced significant land use changes over the centuries, with rangelands being converted into croplands to boost agricultural production. However, this process was later reversed due to land abandonment in the middle of the twentieth century, allowing natural revegetation to take place. As a result, achieving optimal source discrimination in these complex landscapes poses a significant challenge, highlighting the importance of combining different types of tracers.

To explore this possibility, we collected composite source samples from three distinct land uses: cropland, Mediterranean forest, and pine forest, as well as two geomorphic features: degraded areas and channel banks. By considering these diverse sampling locations, we aim to capture the variability in sediment sources within the catchment. Our dataset spans one full hydrological year, allowing us to analyse sediment dynamics throughout different seasons and hydrological events. By integrating isotopic and elemental tracers, we aim to improve the identification and quantification of sediment sources in this intricate catchment setting.

First, the Conservative Balance (CB) method was applied to integrate isotopic ratio and total content of each fatty acid into a single weighted tracer. A substantial improvement of source discrimination was observed when combining the weighted fatty acid (WFA) and elemental composition tracers, compared to their individual usage. Evidence from this study supports the application of different types of tracers when achieving effective discrimination becomes challenging.

The apportionment results revealed that agriculture, channel banks, and subsoils were the primary contributors, accounting for an average contribution of 29%, 39%, and 30% respectively, across most seasons. In contrast, sediment sources characterized by more permanent vegetation cover and minimal human influence, such as the pine afforestation and the Mediterranean forest, exhibited negligible contributions during the studied year. The findings suggest that agricultural practices in Mediterranean agroecosystems, coupled with storm events, play a significant role in the catchment hydrodynamics and subsequently sediment export. Additionally, severe soil loss originating from degraded areas, despite their relatively small coverage, contributes significantly to the overall sediment dynamics.

By unravelling the hydrological implications of these sediment sources, our study provides valuable insights into the interplay between land use, hydrological processes, and sediment dynamics in Mediterranean mountain catchments.

Keywords: Suspended sediment, catchment hydrodynamic, tracer combination, conservative balance method, sediment source discrimination

1. Introduction

The identification of hotspot areas for sediment sources is crucial in recognizing the triggering factors behind the export of fine-grained sediment to streams, where hydrological processes and human activities play a crucial role (Boix-Fayos et al., 2017; Owens, 2020). Inappropriate management practices are responsible for land degradation and the subsequent export of soil sediment and associated nutrients (Ramos et al., 2022). To identify areas prone to erosion and delineate hotspot regions, sediment fingerprinting and spatially distributed erosion models are widely used (Borrelli et al., 2021; Collins et al., 2020). However, even though both methods can be considered complementary, distributed models provide spatial information from areas where erosion is more likely to occur, but they do not inform about the origin of sediments exported to water courses (Lizaga et al., 2022). Contrary to spatially distributed models, sediment fingerprinting techniques deliver information on the origin of sediment. The technique aims to quantify the sediment contribution from each potential source to the mixture or target sample using a variety of tracer properties and quantitative models. However, while sediment fingerprinting has been widely implemented, there still exist open questions regarding the conservative behaviour of tracers, source discrimination power, and especially the tracer selection methods (Evrard et al., 2022). Recent research evidenced that the use of different methods for selecting tracers could substantially modify the apportionment results affecting both Bayesian and Frequentist models (Palazón et al., 2015b; Pulley et al., 2015; Cooper and Krueger, 2017). Other authors devised methodologies to complement fingerprinting studies and developed methods to identify non-conservative, non-consensual, and non-consistent tracers (Lizaga et al. 2020; Latorre et al., 2021). The purpose of these methods is to assess the impact of each individual tracer on the fingerprinting model outputs and determine whether multiple solutions exist within a dataset when applying either Frequentist or Bayesian models for un-mixing. Multiple distinct solutions may arise when working with overdetermined systems characterised by more than n – 1 tracers, being n the number of sources (e.g. 3 sources and 3 or more tracers).

To increase discrimination power and expand the number of potential sources, the use of different types of tracers has been promoted. A wide range of soil properties has been used as fingerprinting tracers during the last decade, such as elemental composition (Ballasus et al., 2022; Derakhshan-Babaei et al., 2022; Dhivert et al., 2022; Liang et al., 2023; Tsyplenkov et al., 2021; Wynants et al., 2020; Zhang et al., 2021), fallout and lithogenic radionuclides combined with stable elements (Navas et al., 2020; Szalińska et al., 2021; Navas et al., 2022; Palazón et al., 2015a; Gaspar et al., 2019), especially ^{137}Cs (Evrard et al., 2020), magnetic properties (Ramon et al., 2020; Zhang et al., 2020) and UV–VIS wavelength absorbance (Lake et al., 2022). However, these properties are mostly not suited to discriminate between different land uses (Hancock and Revill, 2013; Chen et al., 2016). For this reason, plant-specific isotopic signature of organic molecules such as fatty acids (FA) have been proposed for identification of land-use-specific sediment export (Glaser, 2005; Gibbs, 2008; Blake et al., 2012; Alewell et al., 2016; Reiffarth et al., 2016; Mabit et al., 2018; Upadhayay et al., 2018a; Riddle et al., 2022). Since its first use, several studies have implemented isotopes of long-chain fatty acids. The technique has been applied in different environments and setups (Upadhayay et al., 2018b; Lavrieux et al., 2019; Hirave et al., 2020; Lizaga et al., 2021).

When using isotopic tracers, the total tracer content is an essential variable that influences the results (Upadhayay et al 2017). Consequently, concentration-dependent isotopic mixing models are necessary, which hinders their compatibility with elemental tracers. Recently, Lizaga et al. (2022) developed a new physically-based framework, the Conservative Balance (CB) method, that combines isotopic ratio and total content of each fatty acid into a weighted elemental tracer. The CB method presents three benefits: it enables the analysis of isotopic tracers using classical fingerprinting models, it allows the combination of isotopic and elemental tracers directly and, simultaneously, it enables the implementation of advanced tracer selection methods which are key for a correct unmixing process.

Although isotopic tracers have the potential to enhance discrimination among different land uses, they may decrease the discrimination of sources lacking vegetation cover (Reiffarth et al., 2016;

Lizaga et al., 2021). Conversely, elemental composition tracers effectively distinguished geomorphic features but exhibited limitations in discriminating between different vegetation covers. The main shortcoming of the lack of discrimination is the need to combine or remove certain types of sources, or avoid targeting them due to the impossibility of proper source discrimination. The resulting need to exclude or merge sources could represent a limitation when targeting restoration practices, specific vegetation types or geoforms. However, to the best of our knowledge, no study has dealt with a joint implementation of isotopic and elemental tracers to test their ability to discriminate land covers and geomorphic features.

To fill this gap, a dataset composed of the stable isotopic composition of long-chain fatty acids, and elemental composition tracers has been considered to assess the main factors leading to sediment transport during one hydrological year in a mountain Mediterranean catchment with agroforestry practices. Within this context, our analysis and evaluation encompass the following objectives: i) examining the information provided by elemental and isotopic tracers, ii) assessing the impact of combining both tracers, and iii) investigating the primary sources of sediment in relation to rainfall events, land use management, and agricultural activities throughout one hydrological year.

2. Material and methods

2.1 Study area

The study area is a medium size catchment of 23 km^2 located in the northern-central part of the Ebro basin, Spain, with the Barués village in its centre (Fig. 1). An ephemeral stream tributary of the Arba River drains the catchment. The mean annual temperature is 13°C, while the mean annual precipitation ranges between 550 mm to 650 mm (recorded since 1929 at the Yesa reservoir; AEMET). The climate is characterised by cold winters and hot and dry summers when the main streams can dry up. In the last century, the catchment has suffered intense changes in terms of land use and human pressure, varying from agricultural dominance during the 1960s to less than 16%

nowadays (Lizaga et al., 2018a). At present, most of the catchment is occupied by different vegetation covers, with the Mediterranean open forest (MF) and the pine afforestation monoculture (PI) being the predominant types. These covers are interspersed with each other, creating a mosaic habitat with a patch dynamic. The MF occupies 60% of the area, while the PI covers 20% of the area. The remaining 16% is designated as cropland. The Mediterranean forest primarily consists of trees from the *Quercus family*, specifically *Quercus robur* L., *Quercus coccifera* L., and *Quercus ilex* L., as well as scrublands and grasslands. The pine forest, on the other hand, is primarily composed of *Pinus halepensis* Mill., with the main crops being winter cereals such as *Triticum aestivum* L. and *Hordeum vulgare* L.

The soils are alkaline with low organic carbon content and a secondary accumulation of carbonates, mainly classified as Calcisols and Cambisols (IUSS Working Group WRB, 2015) (Lizaga et al., 2019b). The different land uses have predominant silt texture with similar percentage of sand, silt and clay fractions in both the topsoil and deep soil (Lizaga et al., 2018a).

Most of the rainfed agricultural land is located on fluvial terraces occupying the valley floors and the areas close to the streams with gentle slopes (Lizaga et al., 2019a). The valley floor is infilled by eroded sediment from the surrounding slopes and appears deeply incised, especially in the middle and lower parts of the catchment where its thickness reaches its maximum of up to 5 m. The stream channel banks (CB) are mainly composed by silt-dominated colluvium sediment characterised by steep banks without vegetation cover. On the contrary, natural vegetation is located at the highest altitudes, increasing its density from the medium altitudes where the croplands were abandoned in the last years to the upper part where abandonment occurred decades ago. This results in a vertical and horizontal multi-strata canopy structure. Combined with this pattern, the afforestation forest (*Pinus halepensis* Mill.) predominates in most upper Northern parts. The most important crops are winter cereals (*Triticum aestivum* L. and *Hordeum vulgare* L.) with some patches of rapeseed (*Brassica napus* L.). Sowing takes place between October and November, and the harvest season is from mid-May to July.

The precipitation amount was recorded with a one-minute frequency at the study site using a tipping bucket rain gauge connected to an Em50 Decagon data logger. However, some gaps are present in the temporal line due to technical issues. For this reason, data from the Yesa weather station (30T ETRS89 X:648317 Y:4719912, altitude: 487 m.a.s.l), located 20 km north of Barués, were extracted and combined to complete the observed gaps. Previous to the data filling, the relationships between both databases were assessed with an r coefficient of 0.71.

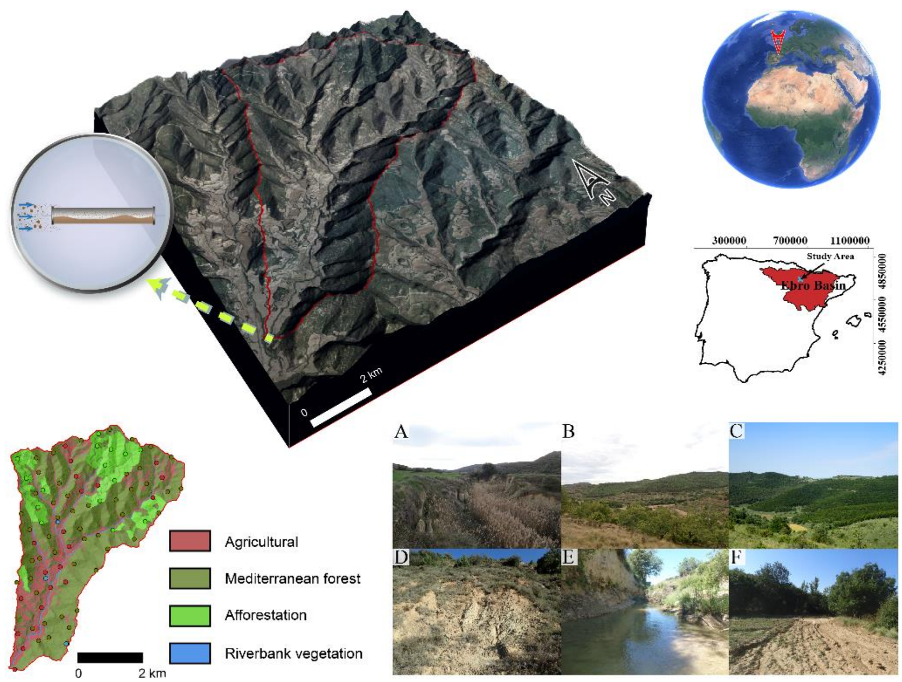

Figure 1. Location of the Barués catchment in the central part of the Ebro Basin (NE Spain). 3D map of the catchment and its surroundings. A-E pictures of the different land use, A) agricultural land use occupying the valley floors and deeply incised stream surrounded by landslides (topples), B) Mediterranean forest, C) pine afforestation, D) degraded soil, E) river bank, and F) eroded crop after a high intensity rainfall.

2.2 Sample collection and analysis

The potential sediment sources and sediment sampling locations established in this study were identified during reconnaissance surveys following previous research conducted in the catchment about hydrological connectivity and coupling (Lizaga et al., 2018b), changes in soil properties after land abandonment (Lizaga et al., 2019b) and ^{137}Cs estimates of spatial soil redistribution rates (Lizaga et al., 2018a).

A total of 130 source samples were collected from the main land uses present in the study catchment. From these, 20 were from cropland (AG), 63 from Mediterranean forest (MF), and 15 from pine afforestation (PI). To analyse the contribution of the main geomorphic elements, 32 source samples were collected from eroded subsoil (SS) areas and main stream channel banks (CB). To evaluate sediment export, suspended sediment collector samples (SSC) were collected following the methodology proposed by Phillips et al. (2000) in the middle part of the stream at the outlet of the catchment. The suspended sediment samples were integrated per three months, and collected as close as possible to the end of each climatological season, during one entire year, from June 2017 to June 2018. The objective of the sampling schedule was to provide a close replication of the suspended sediments transported during each season for evaluating both seasonality and intra-seasonal effects of the crop practices such as sowing, fertilising and harvesting in the sediment contribution to the streams.

Following the predominant silt-loam texture of the soils in the catchment (Lizaga et al., 2021) and the most widespread methodology (Owens et al., 2016), both mixture and source samples were air-dried, ground, homogenised and sieved to ≤63µm particle size. The relationships between tracers and the size fractions support that ≤63µm fraction compile the range of variation for most of the study tracers.

The stable elements and magnetic susceptibility were analysed in the 130 source samples and sediment mixtures. The compound-specific stable isotopes (CSSI) were analysed for a total of 40 source samples and for all the sediment mixtures. A total of 35 tracers were analysed to ensure a variety of fingerprints for characterising the sources and the sediment mixtures. Elemental composition (mg kg^{-1}, Al, As, Bi, Ca, Cr, Cu, Fe, K, Li, Mg, Mn, Mo, Na, Ni, Pb, P, Rb, Se, S, Sr, Ti, Tl, V, Zn) was analysed by ICP-AES after total acid digestion pursued in two cycles with HF (48 %), HNO_3 and H_2O_2 and a second cycle with HNO_3, HCl, and Milli-Q water in a microwave oven. The mass-specific magnetic susceptibility was measured using a Bartington Instruments dual-frequency MS2B sensor in 10 ml samples at low (0.47 kHz; χlf) and high (4.7 kHz; χhf) frequencies. For this study, we use the mean value of three measurements at the low frequency χlf (10^{-8} m3 kg^{-1}).

Lipids were extracted from the soil and sediment (source) and suspended sediment (sink mixture) samples using accelerated solvent extraction (Dionex ASE 350, Thermo Scientific, Bremen Germany) with dichloromethane (DCM): MeOH (9:1 v/v) at 100ºC and 13 MPa in three cycles of 5 min (30 mL cells, 60% flush volume). For this c.a. 3 g of dried sample was weighed in 22 mL stainless steel cells to which a recovery standard was added (12.5 ng C17:0 FA, dissolved in 50 µL ethyl acetate). The recovered C17:0 was used to compute the FA content of the soils and sediments. The lipid extract was dried using rotary evaporation (CentriVap, Labconco, Kansas City, USA) at 60ºC and 20 mbar. Lipid fraction was re-dissolved in DCM/Isopropanol (2:1 v/v) before being separated in neutral and acid fraction using aminopropyl solid-phase extraction columns (Bond Elute, 500mg, 6mL, Agilent Technologies) according to Blake et al. (2012). Neutral fraction was removed with DCM/Isopropanol after which the acid fraction was eluted using 2 % acetic acid in diethyl ether (Russell and Werne, 2007). After taking the acid fraction to dryness by rotary evaporation, the fatty acids were methylated using Methanolic BF_3 (14 %, 20 min at 60 °C).

The obtained fatty acid methyl esters (FAME) were quantified after the addition of an internal standard (C19:0 FAME), using capillary gas chromatography (GC Trace Ultra, Thermo scientific) with flame ionisation detection (FID) equipped with a 5% Phenyl Polysilphenylene-siloxane column (BPX5, 30 m x 0.25 mm x 0.25 µm, Trajan). After adapting the solvent volume for optimal concentration for compound-specific stable isotope (CSSI) analysis, the ^{13}C abundance of the individual FAME was determined using GC-isotope ratio mass spectroscopy (GC-IRMS). The GC-IRMS system used consisted out of a Trace 1310 GC equipped with the same GC column as for GC-FID connected to an ISOLINK II through a CongFlo IV to a Delta-V advantage IRMS detector (All Thermo scientific). Normalisation of the ^{13}C signal on the Vienna Pee Dee belemnite (VPDB) scale was performed by injecting a mixture of C14:0, C16:0, C18:0 C20:0 and C30 FAME, and C14:0, C16:0, C18:0 C20:0 fatty acid ethyl ester provided by Arndt Schimmelmann (Indiana University), calibrated using NBS 19, and L-SVEC defined as exactly +1.95 and -46.6 ‰, on the VPDB scale, respectively, every five samples. Additionally, mixtures of fatty acids (C16, C17, C19 and C20) were methylated together with the samples to correct for the contribution of the methyl group of the FAME in order to obtain the isotopic ratios of the FA.

2.3 Tracer selection methods and fingerprinting model

An essential criterion for tracer selection methods is to exclude non-conservative tracers from being incorporated into the models, as their inclusion may lead to erroneous outcomes (Collins et al., 2017; Haddadchi et al., 2013; Owens et al., 2016; Smith and Blake, 2014). Some tracers fall outside the range of sediment source values due to their lack of conservativeness, sediment particle size effects or external factors such as contamination. Tracer selection is crucial for a successful unmixing and negatively affects all types of models, either Frequentist or Bayesian (Pulley et al., 2015; Cooper and Krueger, 2017; Lizaga et al., 2020a; Latorre et al., 2021).

Additional complexity arises from the joint analysis of isotopic ratios and scalar variables, such as the elemental composition. To this aim, the CB method has been implemented to combine the isotopic ratio and total content of each FA into a weighted tracer that contains the information of both variables. The detailed physical derivation of the CB method can be found in the original research by Lizaga et al. (2022). For the sake of simplicity, the CB method is briefly illustrated using the following equations:

$$\begin{cases} \delta^{13}C = \dfrac{(^{13}C/^{12}C)}{(^{13}C/^{12}C)std} - 1 = \dfrac{\mathrm{R}}{\mathrm{R}std} - 1 \\ C \cong {}^{13}C + {}^{12}C \end{cases} \quad (1)$$

where C represents the carbon total content, R is the isotopic ratio ($^{13}C/^{12}C$) and $\delta^{13}C$ represents the relative difference of isotopic ratios from a standard reference. From the total carbon content (C) and the isotopic ratio (R) of a sample, the individual content of each isotope (^{12}C, ^{13}C) can be derived, being both descriptions equivalent.

$$\begin{cases} {}^{12}C = \dfrac{C}{1+R} \\ {}^{13}C = \dfrac{C \cdot R}{1+R} \end{cases} \tag{2}$$

We now introduce a physical model involving two sediment sources with isotopic contents (C_1, C_2) and isotopic ratios (R_1, R_2) that are mixed into proportions (w_1, w_2), under the constraint $w_1 + w_2 = 1$. The resulting isotope contents in the mixture ($^{12}C_M$, $^{13}C_M$) can be simply calculated by means of a weighted average.

$$\begin{cases} {}^{12}C_M = w_1\,{}^{12}C_1 + w_2\,{}^{12}C_2 \\ {}^{13}C_M = w_1\,{}^{13}C_1 + w_2\,{}^{13}C_2 \end{cases} \tag{3}$$

The first equation in [3], which constitutes the conservative balance of ^{12}C, can be written in terms of C and R using the first equation in [2].

$$\frac{C_M}{1+R_M} = w_1 \frac{C_1}{1+R_1} + w_2 \frac{C_2}{1+R_2} \tag{4}$$

The second equation in [3], which corresponds to the conservative balance of ^{13}C, is expressed in a similar way using the second equation in [2].

$$\frac{C_M R_M}{1+R_M} = w_1 \frac{C_1 R_1}{1+R_1} + w_2 \frac{C_2 R_2}{1+R_2} \tag{5}$$

Both equations, [4] and [5], can be combined by substituting the first term in [4] into Eq. [5].

$$\left(w_1 \frac{C_1}{1+R_1} + w_2 \frac{C_2}{1+R_2}\right) R_M = w_1 \frac{C_1 R_1}{1+R_1} + w_2 \frac{C_2 R_2}{1+R_2} \tag{6}$$

The resulting equation [6] constitutes the conservative balance (CB) of an isotopic tracer and allows calculating the mixture isotopic ratio (R_M) without the need to consider its total content (C_M). As a result, the proposed model retains its validity even when the mixture undergoes physico-chemical processes that may alter its total content while preserving the isotopic ratio.

Starting with Eq. [6], all the terms are shifted to the right side of the equality, and the proportions are factored out.

$$0 = w_1 \frac{C_1(R_1 - R_M)}{1 + R_1} + w_2 \frac{C_2(R_2 - R_M)}{1 + R_2} \tag{7}$$

The resulting equation [7] it is equivalent to the conservative balance of a virtual elemental tracer (T), combining the information of the isotopic ratio and the total content, with the following values in the sources (T_1, T_2) and the mixture (T_M):

$$\begin{cases} T_1 = \dfrac{C_1(R_1 - R_M)}{1 + R_1} \\ T_2 = \dfrac{C_2(R_2 - R_M)}{1 + R_2} \\ T_M = 0 \end{cases} \tag{8}$$

Given the condition that $^{13}C \ll {}^{12}C$ (or equivalently $R \ll 1$) in natural carbon, the precedent expression can be approximated and represented in terms of the measured variables (C, $\delta^{13}C$). Starting with Eq. [7], the numerators are expressed in terms of the relative difference of isotopic ratios ($\delta^{13}C$) substituting the ratio definition, $R=R_{std}(\delta^{13}C+1)$, from equation [1]. The denominators of Eq. [7] are then approximated under the condition $R \ll 1$ using $1+R \cong 1$.

$$0 = w_1 C_1 R_{std}(\delta^{13}C_1 - \delta^{13}C_M) + w_2 C_2 R_{std}(\delta^{13}C_2 - \delta^{13}C_M) \tag{9}$$

The precedent equation is simplified, multiplying both sides of the equality by $1/R_{std}$, and finally expressed as the conservative balance of a virtual elemental tracer (T), obtaining an approximation of Eq. [8] under the condition that R≪1.

$$\begin{cases} T_1 = C_1(\delta^{13}C_1 - \delta^{13}C_M) \\ T_2 = C_2(\delta^{13}C_2 - \delta^{13}C_M) \\ T_M = 0 \end{cases} \tag{10}$$

After this transformation, the isotopic tracers are weighted to scalar quantities and it is possible to implement the Conservativeness Index (CI), Consensus Ranking (CR) and the Consistent Tracer Selection (CTS) methods together with the elemental composition tracers to i) extract the source apportionment predictions that each tracer introduces into the model and identify non-conservative tracers based on that information, ii) unravel the presence of multiple consistent solutions present in over-determined datasets (more or equal number of tracers than sources), and iii) assess the effect of combining elemental and isotopic tracers in source discrimination. CI is a non-parametric test that analyses tracer conservativeness using mixture and source data to create an index as a more sophisticated version of the range test. CR is a scoring function based on several random debates between tracers, in which the tracers preventing consensus are assigned low scores (Lizaga et al., 2020a). Consensus-reaching processes proceed in a convergent multistage way, where experts present their opinions and discuss and negotiate to bring positions closer by modifying their initial opinions (Pérez et al., 2018). In fingerprinting studies, the mentioned experts are the tracers in the dataset. CTS, similar to the DFA, identifies the most discriminant tracers, but it also examines their mathematical properties to ensure consistency in over-determined datasets (e.g., 3 sources and 3 or more tracers) (Latorre et al., 2021).

The CI index was adapted to better describe the conservativeness of tracers in a high-dimensional space of 5 sources. The predicted source contributions from each tracer were first calculated and characterised by its centroid. Then, the CI index was calculated as the percentage of solutions with conservative apportionments ($0 \leq w_i \leq 1$) relative to the centroid position. Thus, while obtaining a similar tracer classification as the previous index, the new definition does not penalise those tracers with dominant apportionments from one source and distributions close to a vertex of the physical space. Despite the new implementation of the CI in the FingerPro R package, both the former and the new definition are available for its comparison.

Based on the mathematical nature of the models, for five sources, a minimum of $n - 1$ tracers are required (being n the number of sources) to obtain a determined system of equations with one possible solution. Thus, a minimum of four tracers are required to unmix five sources. To implement the tracer selection for unmixing, the methods mentioned above were used to remove those tracers with apparently non-conservative or consensual behaviour and select an optimal set of tracers for each mixture. The most discriminant quartet of tracers with a conservative solution extracted from the CTS analysis was extended, incorporating consistent tracers from the dataset with a maximum error threshold $\varepsilon = 0.03$. To estimate the relative contribution of each potential sediment source to the mixtures, a Frequentist fingerprinting model implemented as an R package-FingerPro (Lizaga et al., 2018; Lizaga et al., 2020b) was applied.

3. RESULTS

3.1 The role of each type of tracer and their synergy

To check the discrimination ability, the two types of tracers (weighted δ^{13}C-FA and elemental tracers) were analysed individually and combined. In terms of source discrimination, Fig. 2a-c displays the discriminant capacity of the considered weighted δ^{13}C-FA tracers (δ^{13}C-FAs and FAs-content) using linear discriminant analysis (LDA). The weighted δ^{13}C-FA tracers (WFA) LDA (Fig. 2a) displayed good discrimination between the different land uses such as croplands (AG), Mediterranean forest (Mf) and Pine afforestation (PI), but lower discrimination between the geomorphic features.

Contrary to the WFA tracers, the elemental tracers efficiently discriminated croplands and both geomorphic features while they did not discriminate Mediterranean forest (Mf) and the Pine afforestation (PI). Moreover, a significant enhancement was observed when combining the two types of tracers, exhibiting high discrimination between all sources (Fig. 2c).

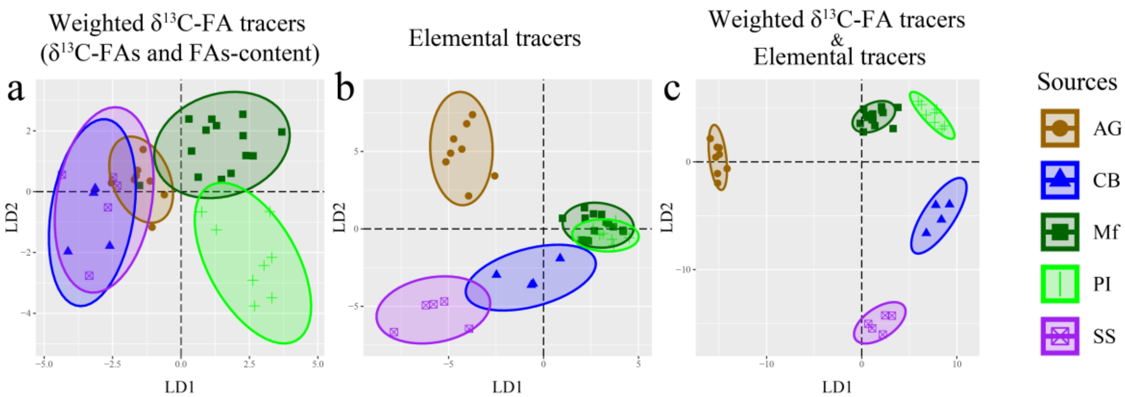

Figure 2. Linear discrimination analysis (LDA) graph of the sediment sources (agricultural - AG, channel bank - CB, Mediterranean forest – Mf, Pine forest - PI and subsoil - SS) for weighted δ^{13}C-FA tracers, elemental tracers and their combination. From left to right: a) weighted δ^{13}C-FA tracer (δ^{13}C-FAs, FAs -Content), b) elemental tracers and c) weighted δ^{13}C-FA tracer combined with elemental tracers.

3.2 Comparing results of weighted δ^{13}C-FA and elemental tracers

The results displayed in Fig. 2 suggest a low discrimination scenario when weighted δ^{13}C-FA (WFA) or elemental tracers are used separately. Following the state-of-the-art when dealing with isotopic signatures, the WFA tracers were unmixed using all long chain fatty acids as tracers. The elemental tracers and the combined datasets were unmixed after selecting the tracers following the CI, CR and CTS methods. The most discriminant and conservative solutions from the elemental tracers and the combination with the WFA tracers were selected and unmixed. As it is illustrated in Fig. 3, and as expected from the discrimination exhibited in Fig. 2, neither the elemental nor the WFA tracers individually produced reliable source apportionments, which was only achieved by combining the WFA and elemental tracers. In Fig. 3a, for example, results from unmixing with the WFA tracers showed a high dispersion and overlap between both geomorphic features (CB and SS) and AG. On the contrary, the unmixing with the elemental tracers (Fig. 3b) showed a defined peak for SS while high variability and overlap between land uses. Finally, the apportionment results from the combined set of tracers (WFA and elemental tracers) (Fig. 3c) displayed well defined and narrow peaks with no significant overlap between the sources.

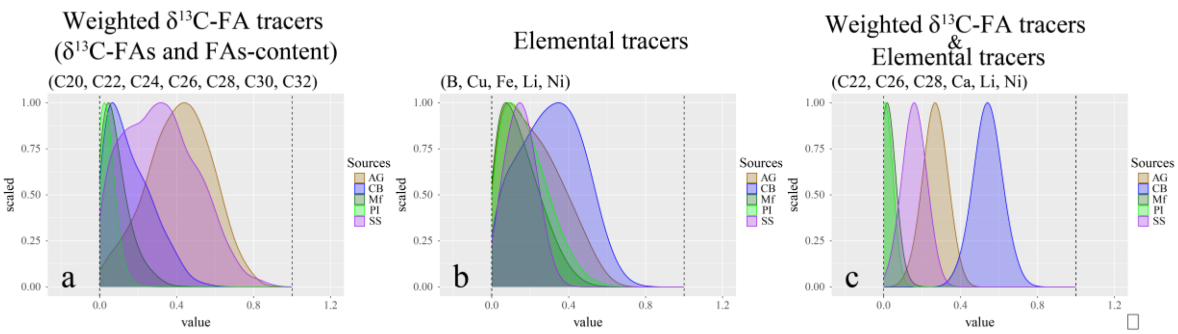

Figure 3. Results of the unmixing procedure for mixture SSC-M1 with weighted δ¹³C-FA tracers (δ¹³C-FAs, FAs-Content), elemental tracers and their combination for the five sediment sources (agricultural - AG, channel bank - CB, Mediterranean forest – Mf, Pine forest - PI and subsoil - SS). From left to right: a) weighted δ¹³C-FA tracer (δ¹³C-FAs, FAs-Content), b) elemental tracers and c) weighted δ¹³C-FA tracer combined with elemental tracers.

3.3 The effect of land management and rainfall on source apportionment changes

The contribution of sources to sediments at the catchment outlet varied seasonally (Fig. 4 and Table S1). The apportionment results for the individual and combined set of tracers displayed in Fig. 4 indicated that channel bank (CB), agriculture (AG) and subsoils (SS) were the main contributors for most seasons with a mean contribution during the entire year of 29%, 39% and 30%, respectively. Sources characterised by a more permanent vegetation cover and low influence of human activities, such as the pine afforestation (PI) and the Mediterranean forest (Mf), showed insignificant contributions for the studied year. Regarding AG, its contribution remained similar during spring and summer (26% and 17%), with a sharp increase after autumn (95%) and decreasing again during winter. In contrast, in winter, a sharp increase of the SS was observed. On the other hand, the CB contribution was high and constant during spring and summer and decreased drastically during autumn and winter. Finally, the SS contribution was most dominant after the winter period (17%).

Table S1. Mean (Avg) and standard deviation (sd) of sediment source contributions obtained via FingerPro model for agricultural (AG), channel bank (CB), Mediterranean forest (Mf), pine forest (PI) and subsoil (SS) to the four seasonal *sediment mixture samples: Spring (SSC-M1), Summer (SSC-M2), Autumn (SSC-M3), and Winter (SSC-M4). CTS, CR and CI refer to the Consistent Tracer Selection (CTS), Consensus Ranking (CR) and Conservativeness Index (CI) methods.*

	AG		CB		Mf		PI		SS		Selected tracers
ID	**Avg**	**sd**	**Avg**	**sd**	**Avg**	**sd**	**Avg**	**sd**	**Avg**	**sd**	**CTS + CR + CI**
Spring (SSC - M 1)	0.26	0.05	0.49	0.09	0.02	0.03	0.00	0.01	0.23	0.10	C22, C26, C28, Ca, Li, Ni
Summer (SSC - M 2)	0.17	0.07	0.46	0.08	0.03	0.03	0.02	0.03	0.32	0.07	C22, C28, C32, Bi, Cr, Ni
Autumn (SSC - M 3)	0.95	0.03	0.02	0.03	0.00	0.01	-0.01	0.00	0.03	0.02	C22, C24, C30, C32, Bi
Winter (SSC - M 4)	0.18	0.04	0.19	0.08	0.02	0.03	0.00	0.01	0.60	0.12	C26, *X*lf, Li, S

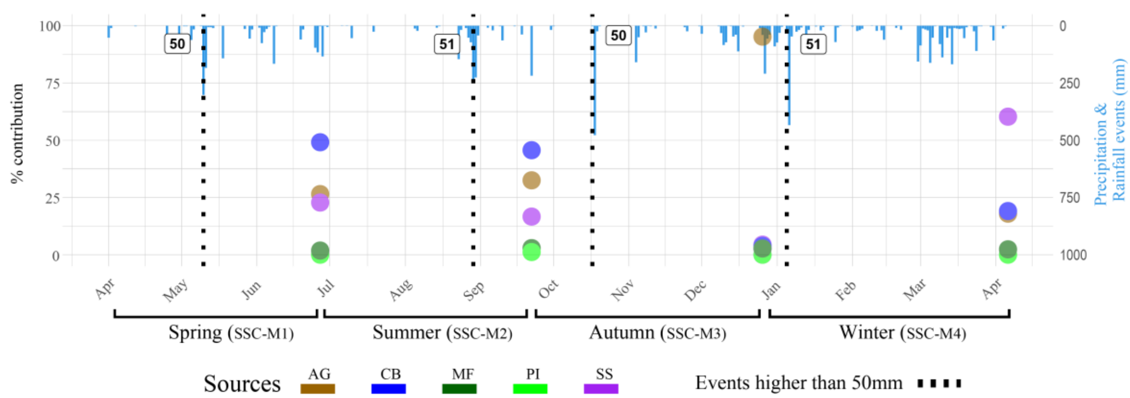

Figure 4. Mean values of sediment source (see Fig. 3 for explanation) proportions (% contribution) during the study period. Vertical black dashed lines highlight rainfall events higher than 50mm with the labels of mm of rainfall in white boxes. The brackets located at the bottom of the graph illustrate the time span since the suspended sediment collector (SSC) was installed and its collection for each season. Spring (SSC-M1), Summer (SSC-M2), Autumn (SSC-M3), and Winter (SSC-M4) represent the four sediment mixtures collected seasonally.

Recorded storm events could prompt source contribution changes such as the one on 2017-10-18, which likely produced the sharp autumn AG peak, or the one on 2018-01-07, which probably triggered the increased contribution of the SS source. The contribution of agricultural (AG) sources exhibited a clear pattern in accordance with the different crop stages with a sharp increase during autumn due to cereal sowing and a noticeable decline as the winter progressed and the crops began to grow. Moreover, this trend is further amplified by the coinciding occurrence of the storm event on October 18, 2017, during a period when most crops are devoid of vegetation and highly susceptible to erosion due to sowing soil disturbance. The absence of vegetation makes the soil more easily erodible, contributing to the heightened impact on agricultural sediment.

4. DISCUSSION

4.1 Highlights and challenges of the tracer combination

Findings from this research confirm previous hypothesis about the benefits of combining long-chain fatty acid and elemental tracers to discriminate different land uses and geomorphic features (Reiffarth et al., 2016; Lizaga et al., 2022). Combining tracers successfully separated and unmixed all sediment sources. As mentioned in previous studies, overlap and large within-source variability of tracer signals are considered important challenges in the application of fingerprinting models (Parnell et al., 2010). This lack of discrimination is likely to result in an increased uncertainty in the estimated source contributions (Phillips and Gregg, 2003; Upadhayay et al., 2017).

Another advantage of combining different types of tracers is that some sources of error, such as low source discrimination or non-conservative processes, could be cancelled due to the selection of alternative tracers. Nevertheless, this improvement in discrimination is at the expense of an increase in complexity. For this reason, informative methods such as the CI, CR and CTS are suggested to implement tracer selection, especially when increasing the number of tracers, resulting in over-determined systems with possible distinct solutions. Thus, employing these informative methods allows for the identification of an optimal set of tracers for each mixture, facilitating accurate fingerprinting results.

Evidences from this study show that tracers with low discrimination capacity, although commonly used in sediment fingerprinting studies (Vale et al., 2022), have a significant impact on the apportionment results and can occasionally lead researchers to incorrect interpretations.

For this reason, developing and validating new techniques to combine different types of tracers is of interest to enhance the accuracy of sediment fingerprinting modelling. The presented issues have not been reported to date for two main reasons: i) it is not common to analyse both types of tracers (isotopic and elemental tracers) in a single study either for budgetary reasons or equipment availability and ii) the lack of a method to combine δ^{13}C-FAs and FAs-content into a weighted elemental tracer.

4.2 Triggering factors of changes in sediment export

The results from this research identify soil degradation mainly due to poor past land management and overgrazing and present agricultural practices as main drivers for source contribution changes in the study catchment. Recent studies combining remote sensing and particle size analysis have shed light on the relationship between rainfall, vegetation status, and stage on particle size variations and exported mass (Lizaga et al., 2022b). While rainfall remains the predominant factor, the vegetation status and crop stage also exert influence on the particle size and exported mass. In line with this previous evidence, our results support that land use management and human impacts make sediments available so that after the occurrence of rainfall events, sediments are washed away by runoff in the sediment cascade within the hydrological system to be finally exported downstream. This trend follows the general crop stages, with the highest contribution from the AG source in autumn due to sowing of winter cereals and the bare soil surface. During the spring and summer seasons, the contribution of channel banks (CB) remains consistently high as they serve as the closest available sediment source. However, in autumn, their contribution experiences a significant decrease due to the dominant input from agricultural (AG) sources, which obscures the signals from other sources. In winter, the CB contribution is also reduced due to the overall stability and limited disturbance of the surrounding areas, mainly characterised by the presence of croplands. This consistent relationship between CB and AG contributions throughout most of the year can be attributed to the strategic location of most croplands. These croplands are typically situated on fluvial terraces occupying the valley floors surrounding the streams. The choice of this location for cultivating crops is influenced by factors such as accessibility, the absence of steep slopes, and the presence of deeper soils (refer to Fig. 1A). Thus, every process induced by the agricultural practices close to the borders of the channel banks could facilitate piping or other erosion processes that lead to rainfall-induced topless or landslides of the almost vertical channel banks. This phenomenon becomes particularly evident under intense storm events, as observed by Gaspar et al. (2019) during an exceptional storm event in October 2012. Despite the high sediment export from agricultural sources, the CB stood out as the primary contributor. This was primarily due to the sharp increase in erosive processes triggered by the shear stress on the banks across the entire talus section which are the closest available sediment source (Lizaga et al., 2019a).

As previously discussed, the presence of vegetation growth in croplands plays a crucial role in stabilising channel banks throughout the year, except during extreme rainfall events. This vegetation cover, coupled with the absence of tillage practices and the growth of crops, leads to a relatively moderate to low contribution from both channel banks and croplands during the winter period. During this time, numerous rainfall events of moderate intensity occur, causing erosion primarily in degraded areas while having limited impact on the croplands or channel banks. Consequently, the primary source of sediment during the winter period shifts to bare soil or degraded areas (referred to as SS), surpassing contributions from other sources.

The low contribution of MF and PI sources is determined by the protective effect of the vegetation cover, further enhanced by the terraced landscaped characteristic in the pine afforestation areas, which agrees with observations in other environments (Bravo-Linares et al., 2018; Gibbs, 2008). Likely, only extreme storm events that overflow the pine terraces have the capability to mobilise surface soil from these well-protected surfaces and transport it into the main streams. However, during these events, the amount of sediment exported is still insignificant compared to the high contribution from the other sources (Lizaga et al., 2019a). Nevertheless, previous studies conducted in the area have identified a significant increase in sediment contributions from the pine forests as a result of clearcutting activities. This is primarily attributed to the presence of bare soil left behind during the clearcutting process and the subsequent traffic of heavy machinery (Lizaga et al., 2021). These factors contribute to an elevated sediment supply from the clearcut areas of harvested pine forests which were not detected during the study period.

5. CONCLUSIONS

Despite the complexity of the study area and its homogeneous lithology, the combined use of weighted fatty acids (δ^{13}C-FAs and FAs-content) and elemental composition tracers successfully identified the five sediment sources for seasonally collected suspended sediments. In contrast, the individual use of either weighted fatty acids or elemental tracers produced inconsistent results for this specific study. Therefore, employing multiple types of tracers in complex catchments is crucial to reach a consensus and facilitate the identification of specific sources that would otherwise be indistinguishable, despite their potentially significant contributions. Careful consideration should be given when unmixing a large number of sources (> 4 sources) in complex environments to avoid over/underestimation of sparsely discriminated sources.

The results of this research highlight the dominant role of agricultural practices and high storm events in driving the spatiotemporal variability of sediment export. Apportionment results provide evidence of the severe soil loss caused by land degradation and the impact of bare soil in Mediterranean agroecosystems despite its relatively small surface coverage. These findings suggest the possibility of implementing targeted restoration strategies without sacrificing the identification of sediment provenance from geoforms or land covers. By encompassing multiple potential sources and obtaining more precise results, this methodology opens up opportunities for the implementation and monitoring of targeted restoration strategies with greater efficacy.

The presented methods have been implemented in the R programming language and will be published in the Comprehensive R Archive Network (CRAN) and GitHub repositories within the FingerPro package. Furthermore, in adherence to the FAIR principles (findability, accessibility, interoperability, and reuse), the data required to replicate the results and figures presented in this manuscript will be made available on a public repository.

ACKNOWLEDGEMENTS

This research is part of the Project I+D+i PID 2019-104857RB-I00, funded by the MCIN/AEI/10.13039/501100011033/ and the aid of a predoctoral contract BES-2015-071780 of the project CGL2014-52986-R. The contribution of IL was supported by the Research Foundation-Flanders (FWO, mandate 12V8622N).

REFERENCES

Alewell, Christine, Birkholz, A., Meusburger, K., Schindler Wildhaber, Y., Mabit, L., 2016. Quantitative sediment source attribution with compound-specific isotope analysis in a C3 plant-dominated catchment (central Switzerland). Biogeosciences 13, 1587–1596. https://doi.org/10.5194/bg-13-1587-2016

Alewell, C., Birkholz, A., Meusburger, K., Schindler Wildhaber, Y., Mabit, L., 2016. Quantitative sediment source attribution with compound-specific isotope analysis in a C3 plant-dominated catchment (central Switzerland). Biogeosciences 13, 1587–1596. https://doi.org/10.5194/bg-13-1587-2016

Ballasus, H., Schneider, B., von Suchodoletz, H., Miera, J., Werban, U., Fütterer, P., Werther, L., Ettel, P., Veit, U., Zielhofer, C., 2022. Overbank silt-clay deposition and intensive Neolithic land use in a Central European catchment – Coupled or decoupled? Sci. Total Environ. 806, 150858. https://doi.org/10.1016/j.scitotenv.2021.150858

Blake, W.H., Ficken, K.J., Taylor, P., Russell, M.A., Walling, D.E., 2012. Tracing crop-specific sediment sources in agricultural catchments. Geomorphology 139, 322–329. https://doi.org/10.1016/j.geomorph.2011.10.036

Boix-Fayos, C., Martínez-Mena, M., Cutillas, P.P., de Vente, J., Barberá, G.G., Mosch, W., Navarro Cano, J.A., Gaspar, L., Navas, A., 2017. Carbon redistribution by erosion processes in an intensively disturbed catchment. CATENA, Geoecology in

Mediterranean mountain areas. Tribute to Professor José María García Ruiz 149, 799–809. https://doi.org/10.1016/j.catena.2016.08.003

Borrelli, P., Alewell, C., Alvarez, P., Anache, J.A.A., Baartman, J., Ballabio, C., Bezak, N., Biddoccu, M., Cerdà, A., Chalise, D., Chen, S., Chen, W., De Girolamo, A.M., Gessesse, G.D., Deumlich, D., Diodato, N., Efthimiou, N., Erpul, G., Fiener, P., Freppaz, M., Gentile, F., Gericke, A., Haregeweyn, N., Hu, B., Jeanneau, A., Kaffas, K., Kiani-Harchegani, M., Villuendas, I.L., Li, C., Lombardo, L., López-Vicente, M., Lucas-Borja, M.E., Märker, M., Matthews, F., Miao, C., Mikoš, M., Modugno, S., Möller, M., Naipal, V., Nearing, M., Owusu, S., Panday, D., Patault, E., Patriche, C.V., Poggio, L., Portes, R., Quijano, L., Rahdari, M.R., Renima, M., Ricci, G.F., Rodrigo-Comino, J., Saia, S., Samani, A.N., Schillaci, C., Syrris, V., Kim, H.S., Spinola, D.N., Oliveira, P.T., Teng, H., Thapa, R., Vantas, K., Vieira, D., Yang, J.E., Yin, S., Zema, D.A., Zhao, G., Panagos, P., 2021. Soil erosion modelling: A global review and statistical analysis. Sci. Total Environ. 146494. https://doi.org/10.1016/j.scitotenv.2021.146494

Bravo-Linares, C., Schuller, P., Castillo, A., Ovando-Fuentealba, L., Muñoz-Arcos, E., Alarcón, O., de los Santos-Villalobos, S., Cardoso, R., Muniz, M., Meigikos dos Anjos, R., Bustamante-Ortega, R., Dercon, G., 2018. First use of a compound-specific stable isotope (CSSI) technique to trace sediment transport in upland forest catchments of Chile. Sci. Total Environ. 618, 1114–1124. https://doi.org/10.1016/j.scitotenv.2017.09.163

Chen, F., Fang, N., Shi, Z., 2016. Using biomarkers as fingerprint properties to identify sediment sources in a small catchment. Sci. Total Environ. 557–558, 123–133. https://doi.org/10.1016/j.scitotenv.2016.03.028

Collins, A.L., Blackwell, M., Boeckx, P., Chivers, C.-A., Emelko, M., Evrard, O., Foster, I., Gellis, A., Gholami, H., Granger, S., Harris, P., Horowitz, A.J., Laceby, J.P., Martinez-Carreras, N., Minella, J., Mol, L., Nosrati, K., Pulley, S., Silins, U., da Silva, Y.J., Stone, M., Tiecher, T., Upadhayay, H.R., Zhang, Y., 2020. Sediment source fingerprinting: benchmarking recent outputs, remaining challenges and emerging themes. J. Soils Sediments 20, 4160–4193. https://doi.org/10.1007/s11368-020-02755-4

Cooper, R.J., Krueger, T., 2017. An extended Bayesian sediment fingerprinting mixing model for the full Bayes treatment of geochemical uncertainties. Hydrol. Process. 31, 1900–1912. https://doi.org/10.1002/hyp.11154

Cooper, R.J., Pedentchouk, N., Hiscock, K.M., Disdle, P., Krueger, T., Rawlins, B.G., 2015. Apportioning sources of organic matter in streambed sediments: An integrated molecular and compound-specific stable isotope approach. Sci. Total Environ. 520, 187–197. https://doi.org/10.1016/j.scitotenv.2015.03.058

Derakhshan-Babaei, F., Mirchooli, F., Mohammadi, M., Nosrati, K., Egli, M., 2022. Tracking the origin of trace metals in a watershed by identifying fingerprints of soils, landscape and river sediments. Sci. Total Environ. 835, 155583. https://doi.org/10.1016/j.scitotenv.2022.155583

Dhivert, E., Dendievel, A.-M., Desmet, M., Devillers, B., Grosbois, C., 2022. Hydro-sedimentary dysfunctions as a key factor for the storage of contaminants in mountain rivers (Bienne River, Jura Mountains, France). CATENA 213, 106122. https://doi.org/10.1016/j.catena.2022.106122

Evrard, O., Batista, P.V.G., Company, J., Dabrin, A., Foucher, A., Frankl, A., García-Comendador, J., Huguet, A., Lake, N., Lizaga, I., Martínez-Carreras, N., Navratil, O., Pignol, C., Sellier, V., 2022. Improving the design and implementation of sediment fingerprinting studies: summary and outcomes of the TRACING 2021 Scientific School. J. Soils Sediments. https://doi.org/10.1007/s11368-022-03203-1

Evrard, O., Chaboche, P.-A., Ramon, R., Foucher, A., Laceby, J.P., 2020. A global review of sediment source fingerprinting research incorporating fallout radiocesium (137Cs). Geomorphology 362, 107103. https://doi.org/10.1016/j.geomorph.2020.107103

Gaspar, L., Lizaga, I., Blake, W.H., Latorre, B., Quijano, L., Navas, A., 2019. Fingerprinting changes in source contribution for evaluating soil response during an exceptional rainfall in Spanish pre-pyrenees. J. Environ. Manage. 240, 136–148. https://doi.org/10.1016/j.jenvman.2019.03.109

Gibbs, M.M., 2008. Identifying Source Soils in Contemporary Estuarine Sediments: A New Compound-Specific Isotope Method. Estuaries Coasts 31, 344–359. https://doi.org/10.1007/s12237-007-9012-9

Glaser, B., 2005. Compound-specific stable-isotope (δ13C) analysis in soil science. J. Plant Nutr. Soil Sci. 168, 633–648. https://doi.org/10.1002/jpln.200521794

Hancock, G.J., Revill, A.T., 2013. Erosion source discrimination in a rural Australian catchment using compound-specific isotope analysis (CSIA). Hydrol. Process. 27, 923–932. https://doi.org/10.1002/hyp.9466

Hirave, P., Glendell, M., Birkholz, A., Alewell, C., 2020. Compound-specific isotope analysis with nested sampling approach detects spatial and temporal variability in the sources of suspended sediments in a Scottish mesoscale catchment. Sci. Total Environ. 142916. https://doi.org/10.1016/j.scitotenv.2020.142916

ilizaga, 2018. eead-csic-eesa/fingerPro_model: fingerPro 1.1. https://doi.org/10.5281/zenodo.1402029

Lake, N.F., Martínez-Carreras, N., Shaw, P.J., Collins, A.L., 2022. High frequency un-mixing of soil samples using a submerged spectrophotometer in a laboratory setting—implications for sediment fingerprinting. J. Soils Sediments 22, 348–364. https://doi.org/10.1007/s11368-021-03107-6

Latorre, B., Lizaga, I., Gaspar, L., Navas, A., 2021. A novel method for analysing consistency and unravelling multiple solutions in sediment fingerprinting. Sci. Total Environ. 789, 147804. https://doi.org/10.1016/j.scitotenv.2021.147804

Lavrieux, M., Birkholz, A., Meusburger, K., Wiesenberg, G.L.B., Gilli, A., Stamm, C., Alewell, C., 2019. Plants or bacteria? 130 years of mixed imprints in Lake Baldegg sediments (Switzerland), as revealed by compound-specific isotope analysis (CSIA) and biomarker analysis. Biogeosciences 16, 2131–2146. https://doi.org/10.5194/bg-16-2131-2019

Liang, A., Zhang, Z., Lizaga, I., Dong, Z., Zhang, Y., Liu, X., Xiao, F., Gao, J., 2023. Which is the dominant source for the aeolian sand in the Badain Jaran Sand Sea, Northwest China: Fluvial or gobi sediments? CATENA 225, 107011. https://doi.org/10.1016/j.catena.2023.107011

Lizaga, I., Bodé, S., Gaspar, L., Latorre, B., Boeckx, P., Navas, A., 2021. Legacy of historic land cover changes on sediment provenance tracked with isotopic tracers in a Mediterranean agroforestry catchment. J. Environ. Manage. 288, 112291. https://doi.org/10.1016/j.jenvman.2021.112291

Lizaga, I., Gaspar, L., Blake, W.H., Latorre, B., Navas, A., 2019a. Fingerprinting changes of source apportionments from mixed land uses in stream sediments before and after an exceptional rainstorm event. Geomorphology 341, 216–229. https://doi.org/10.1016/j.geomorph.2019.05.015

Lizaga, I., Latorre, B., Gaspar, L., Navas, A., 2022a. Effect of historical land-use change on soil erosion in a Mediterranean catchment by integrating 137Cs measurements and WaTEM/SEDEM model. Hydrol. Process. 36, e14577. https://doi.org/10.1002/hyp.14577

Lizaga, I., Latorre, B., Gaspar, L., Navas, A., 2022b. Combined use of geochemistry and compound-specific stable isotopes for sediment fingerprinting and tracing. Sci. Total Environ. 154834. https://doi.org/10.1016/j.scitotenv.2022.154834

Lizaga, I., Latorre, B., Gaspar, L., Navas, A., 2020a. Consensus ranking as a method to identify non-conservative and dissenting tracers in fingerprinting studies. Sci. Total Environ. 720, 137537. https://doi.org/10.1016/j.scitotenv.2020.137537

Lizaga, I., Latorre, B., Gaspar, L., Navas, A., 2020b. FingerPro: an R Package for Tracking the Provenance of Sediment. Water Resour. Manag. 34, 3879–3894. https://doi.org/10.1007/s11269-020-02650-0

Lizaga, I., Quijano, L., Gaspar, L., Navas, A., 2018a. Estimating soil redistribution patterns with 137Cs measurements in a Mediterranean mountain catchment affected by land abandonment. Land Degrad. Dev. 29, 105–117. https://doi.org/10.1002/ldr.2843

Lizaga, I., Quijano, L., Gaspar, L., Ramos, M.C., Navas, A., 2019b. Linking land use changes to variation in soil properties in a Mediterranean mountain agroecosystem. CATENA 172, 516–527. https://doi.org/10.1016/j.catena.2018.09.019

Lizaga, I., Quijano, L., Palazón, L., Gaspar, L., Navas, A., 2018b. Enhancing Connectivity Index to Assess the Effects of Land Use Changes in a Mediterranean Catchment. Land Degrad. Dev. 29, 663–675. https://doi.org/10.1002/ldr.2676

Mabit, L., Gibbs, M., Mbaye, M., Meusburger, K., Toloza, A., Resch, C., Klik, A., Swales, A., Alewell, C., 2018. Novel application of Compound Specific Stable Isotope (CSSI) techniques to investigate on-site sediment origins across arable fields. Geoderma 316, 19–26. https://doi.org/10.1016/j.geoderma.2017.12.008

Navas, A., Lizaga, I., Gaspar, L., Latorre, B., Dercon, G., 2020. Unveiling the provenance of sediments in the moraine complex of Aldegonda Glacier (Svalbard) after glacial retreat using radionuclides and elemental fingerprints. Geomorphology 367, 107304. https://doi.org/10.1016/j.geomorph.2020.107304

Navas, A., Lizaga, I., Santillán, N., Gaspar, L., Latorre, B., Dercon, G., 2022. Targeting the source of fine sediment and associated geochemical elements by using novel fingerprinting methods in proglacial tropical highlands (Cordillera Blanca, Perú). Hydrol. Process. 36, e14662. https://doi.org/10.1002/hyp.14662

Owens, P.N., 2020. Soil erosion and sediment dynamics in the Anthropocene: a review of human impacts during a period of rapid global environmental change. J. Soils Sediments 20, 4115–4143. https://doi.org/10.1007/s11368-020-02815-9

Palazón, L., Gaspar, L., Latorre, B., Blake, W.H., Navas, A., 2015a. Identifying sediment sources by applying a fingerprinting mixing model in a Pyrenean drainage catchment. J. Soils Sediments 15, 2067–2085. https://doi.org/10.1007/s11368-015-1175-6

Palazón, L., Latorre, B., Gaspar, L., Blake, W.H., Smith, H.G., Navas, A., 2015b. Comparing catchment sediment fingerprinting procedures using an auto-evaluation approach with virtual sample mixtures. Sci. Total Environ. 532, 456–466. https://doi.org/10.1016/j.scitotenv.2015.05.003

Parnell, A.C., Inger, R., Bearhop, S., Jackson, A.L., 2010. Source Partitioning Using Stable Isotopes: Coping with Too Much Variation. PLOS ONE 5, e9672. https://doi.org/10.1371/journal.pone.0009672

Phillips, D.L., Gregg, J.W., 2003. Source partitioning using stable isotopes: coping with too many sources. Oecologia 136, 261–269. https://doi.org/10.1007/s00442-003-1218-3

Pulley, S., Foster, I., Antunes, P., 2015. The uncertainties associated with sediment fingerprinting suspended and recently deposited fluvial sediment in the Nene river basin. Geomorphology 228, 303–319. https://doi.org/10.1016/j.geomorph.2014.09.016

Ramon, R., Evrard, O., Laceby, J.P., Caner, L., Inda, A.V., Barros, C.A.P. de, Minella, J.P.G., Tiecher, T., 2020. Combining spectroscopy and magnetism with geochemical tracers to improve the discrimination of sediment sources in a homogeneous subtropical catchment. CATENA 195, 104800. https://doi.org/10.1016/j.catena.2020.104800

Reiffarth, D.G., Petticrew, E.L., Owens, P.N., Lobb, D.A., 2016. Sources of variability in fatty acid (FA) biomarkers in the application of compound-specific stable isotopes (CSSIs) to soil and sediment fingerprinting and tracing: A review. Sci. Total Environ. 565, 8–27. https://doi.org/10.1016/j.scitotenv.2016.04.137

Riddle, B., Fox, J., Mahoney, D.T., Ford, W., Wang, Y.-T., Pollock, E., Backus, J., 2022. Considerations on the use of carbon and nitrogen isotopic ratios for sediment fingerprinting. Sci. Total Environ. 817, 152640. https://doi.org/10.1016/j.scitotenv.2021.152640

Szalińska, E., Zemełka, G., Kryłów, M., Orlińska-Woźniak, P., Jakusik, E., Wilk, P., 2021. Climate change impacts on contaminant loads delivered with sediment yields from different land use types in a Carpathian basin. Sci. Total Environ. 755, 142898. https://doi.org/10.1016/j.scitotenv.2020.142898

Tsyplenkov, A., Vanmaercke, M., Collins, A.L., Kharchenko, S., Golosov, V., 2021. Elucidating suspended sediment dynamics in a glacierised catchment after an exceptional erosion event: The Djankuat catchment, Caucasus Mountains, Russia. CATENA 203, 105285. https://doi.org/10.1016/j.catena.2021.105285

Upadhayay, H.R., Bodé, S., Griepentrog, M., Bajracharya, R.M., Blake, W., Cornelis, W., Boeckx, P., 2018a. Isotope mixing models require individual isotopic tracer content for correct quantification of sediment source contributions. Hydrol. Process. 32, 981–989.

Upadhayay, H.R., Bodé, S., Griepentrog, M., Huygens, D., Bajracharya, R.M., Blake, W.H., Dercon, G., Mabit, L., Gibbs, M., Semmens, B.X., Stock, B.C., Cornelis, W., Boeckx, P., 2017. Methodological perspectives on the application of compound-specific stable isotope fingerprinting for sediment source apportionment. J. Soils Sediments 1537–1553.

Upadhayay, H.R., Smith, H.G., Griepentrog, M., Bodé, S., Bajracharya, R.M., Blake, W., Cornelis, W., Boeckx, P., 2018b. Community managed forests dominate the catchment sediment cascade in the mid-hills of Nepal: A compound-specific stable isotope analysis. Sci. Total Environ. 637–638, 306–317. https://doi.org/10.1016/j.scitotenv.2018.04.394

Vale, S., Swales, A., Smith, H.G., Olsen, G., Woodward, B., 2022. Impacts of tracer type, tracer selection, and source dominance on source apportionment with sediment fingerprinting. Sci. Total Environ. 831, 154832. https://doi.org/10.1016/j.scitotenv.2022.154832

Wynants, M., Millward, G., Patrick, A., Taylor, A., Munishi, L., Mtei, K., Brendonck, L., Gilvear, D., Boeckx, P., Ndakidemi, P., Blake, W.H., 2020. Determining tributary sources of increased sedimentation in East-African Rift Lakes. Sci. TOTAL Environ. 717.

Zhang, J., Yang, M., Zhang, F., Tang, Y., Wang, X., Wang, Y., 2020. Revealing soil erosion characteristics using deposited sediment sources in a complex small catchment in the wind-water erosion crisscross region of the Chinese Loess Plateau. Geoderma 379, 114634. https://doi.org/10.1016/j.geoderma.2020.114634

Zhang, Z., Liang, A., Zhang, C., Dong, Z., 2021. Gobi deposits play a significant role as sand sources for dunes in the Badain Jaran Desert, Northwest China. CATENA 206, 105530. https://doi.org/10.1016/j.catena.2021.105530

Figure captions

Figure 3. Location of the Barués catchment in the central part of the Ebro Basin (NE Spain). 3D map of the catchment and its surroundings. A-E pictures of the different land use, A) agricultural land use occupying the valley floors and deeply incised stream surrounded by landslides (topples), B) Mediterranean forest, C) pine afforestation, D) degraded soil, E) river bank, and F) eroded crop after a high intensity rainfall.

Figure 4. Linear discrimination analysis (LDA) graph of the sediment sources (agricultural - AG, channel bank - CB, Mediterranean forest – Mf, Pine forest - PI and subsoil - SS) for weighted δ13C-FA tracers, elemental tracers and their combination. From left to right: a) weighted δ13C-FA tracer (δ13C-FAs, FAs -Content), b) elemental tracers and c) weighted δ13C-FA tracer combined with elemental tracers.

Figure 3. Results of the unmixing procedure for mixture SSC-M1 with weighted δ13C-FA tracers (δ13C-FAs, FAs-Content), elemental tracers and their combination for the five sediment sources (agricultural - AG, channel bank - CB, Mediterranean forest – Mf, Pine forest - PI and subsoil - SS). From left to right: a) weighted δ13C-FA tracer (δ13C-FAs, FAs-Content), b) elemental tracers and c) weighted δ13C-FA tracer combined with elemental tracers.

Figure 4. Mean values of sediment source (see Fig. 3 for explanation) proportions (% contribution) during the study period. Vertical black dashed lines highlight rainfall events higher than 50mm with the labels of mm of rainfall in white boxes. The brackets located at the bottom of the graph illustrate the time span since the suspended sediment collector (SSC) was installed and its collection for each season. Spring (SSC-M1), Summer (SSC-M2), Autumn (SSC-M3), and Winter (SSC-M4) represent the four sediment mixtures collected seasonally.